J. Braz. Chem. Soc., Vol. 21, No. 9, 1704-1709, 2010.
Printed in Brazil - ©2010 Sociedade Brasileira de Química
0103 - 5053 $6.00+0.00

Article

Macroporous MnO_2 Electrodes Obtained by Template Assisted Electrodeposition for Electrochemical Capacitors

Tânia M. Benedetti, Vinicius R. Gonçales, Denise F. S. Petri, Susana I. Córdoba de Torresi and Roberto M. Torresi*

Instituto de Química, Universidade de São Paulo, CP 26077, 05513-970 São Paulo-SP, Brazil

Eletrodos macroporosos de MnO_2 foram preparados por eletrodeposição assistida por molde de partículas esféricas coloidais de poliestireno. A molhabilidade desses filmes foi estudada por medidas de ângulo de contato. Medidas de voltametria cíclica foram realizadas com o objetivo de estudar o seu comportamento como eletrodo para supercapacitores. A capacitância específica obtida foi cerca de 60% maior que a obtida por um eletrodo liso, o que mostra que apesar de a molhabilidade do eletrodo macroporoso ser menor, ocorre alguma penetração do eletrólito pelos poros, aumentando a área eletroativa. Por fim, o eletrodo macroporoso apresentou excelente estabilidade eletroquímica, não sendo observada queda de capacitância após 1000 ciclos de carga e descarga.

Macroporous MnO_2 electrodes prepared by template-assisted electrodeposition using spherical polystyrene colloidal particles are studied. The wettability of such electrodes by a $LiClO_4$ aqueous electrolyte is measured by the contact angle technique. Cyclic voltammetry experiments are performed in order to evaluate the use of these electrodes for electrochemical capacitor applications. The specific capacity obtained is about 60% higher than that obtained for flat MnO_2 surfaces showing that, in spite of the wettability being lower, some penetration of the electrolyte into the pores must occur, increasing the electroactive area with respect to the flat electrode. Furthermore, the macroporous electrode showed excellent electrochemical stability, with neither a capacitance decrease nor a loss of morphology, after 1000 cycles.

Keywords: supercapacitors, manganese oxide, porous electrodes, template assisted electro deposition, wettability

Introduction

Li-ion batteries are widely used as energy sources for portable electronic devices, and several studies have been carried out in order to improve their performance.[1] As charge/discharge processes are limited by reaction kinetics,[2] the search for devices that can deliver high power is an active field. Electrochemical capacitors or supercapacitors are high power sources that can be fully charged/discharged in seconds because they are based on surface faradaic reactions and/or double-layer capacitance.[3,4] These devices can be applied together with a battery in order to allow both high energy and power or to replace conventional capacitors based on electrical charge separation. The preparation of high surface area electrodes can improve device performance because more material is available on the surface for charge compensation as well as for energy storage.[2]

Concerning redox-active materials for supercapacitors, RuO_2 presents the best capacitance values. However, its high cost does not allow its use in practical applications.[5] An alternative low cost, non toxic and environmentally friend material is MnO_2.[6-9] The electrochemical performance of MnO_2-based supercapacitors and the mechanism of energy storage depend on several aspects, such as morphology,[10,11] structure[12,13] and post synthesis thermal treatment.[14] The major interest is to use MnO_2 as positive electrode together with carbon as negative electrode in hybrid systems, improving the cell voltage, thus, improving energy and power densities.[15]

In a previous work[16] the obtention of macroporous MnO_2 electrodes has been briefly reported together with the preparation of other electroactive porous thin films, showing the potential application of the methodology.

*e-mail: rtorresi@iq.usp.br

This technique allows the obtention of uniform films with a very narrow porous diameter distribution because the compounds are electrodeposited between the template voids and around the surface of the colloidal particles. This method also allows good mass and thickness control through the applied charge.[17,18] As there is no shrinkage of the material when the template is removed, the resulting film is a true cast of the template structure.

In this paper, the wettability and electrochemical performance of macroporous and massive MnO_2 films have been studied by contact angle (CA) measurements and cyclic voltammetry (CV), respectively. The goal of the present study is to verify the aspects concerning the use of pores to increase the specific area of the electrode for supercapacitor applications.

Experimental

Chemicals

Triton X-100 (tetra-octylfenoxypolyetoxyethanol), polystyrene latex particles, at 10% wt. dispersion in water, with a 460 nm diameter, potassium permanganate and lithium perchlorate (Aldrich) were used without further purification. The solutions were prepared with 18 MΩ cm^{-1} water purified by an Elga UHQ system.

Instrumental

For FESEM images, a field emission scanning electron microscope (FESEM, JSM-7401F from JEOL) was employed. CA measurements were performed by using a home built apparatus.[18] Electrochemical data were obtained with a potentiostat/galvanostat Autolab model PGSTAT 30 (Eco Chemie), and, in order to obtain the mass of MnO_2 films, an electrochemical quartz crystal microbalance (EQCM) consisting of a Stanford Research System model SR620 frequency meter connected to an oscillating circuit was used. As the substrate, 6.0 MHz AT-cut overtone polished piezoelectric quartz crystals (Valpey – Fischer) with a 25 mm diameter and 0.32 cm^2 gold piezoactive electrode area (integral sensitive factor 6.45×10^7 cm^2 Hz g^{-1}) were used.

The X-ray absorption data were collected in the fluorescence mode in the K-edge of Mn. Measurements were conducted at the XAS beam line of the National Synchrotron Light Source (LNLS), Brazil. The computer program used for the analysis of the X-ray absorption data was the Athena package. The x-ray absorption near-edge spectroscopy (XANES) spectra were first corrected for background absorption by fitting the pre-edge data (from –60 to –20 eV below the edge) to a linear formula, followed by extrapolation and subtraction from the data over the energy range of interest. Next, the spectra were calibrated for the edge position using the second derivative of the inflection point at the edge jump of the data. Finally, the spectra were normalized taken as reference the inflection point of one of the EXAFS oscillations.

MnO_2 macroporous film preparation

The assembly of polystyrene nanospheres as well as the electrodeposition of MnO_2 was performed according to the literature.[16] Briefly, two additions of 20 μL of 0.5% wt. polystyrene nanospheres, with a 460 nm diameter and suspended in a 10^{-6} mol L^{-1} Triton X-100 aqueous solution, were added over the gold substrate and dried slowly at room temperature. Next, a thermal treatment at 100 °C was performed for 4 h in order to produce a mechanically stable template over the electrode. Then, a MnO_2 film was obtained by galvanostatic electrodeposition from a 0.02 mol L^{-1} $KMnO_4$ aqueous solution by applying a cathodic current density of 750 μA cm^{-2} for 2 min. The geometric area has been considered. Before the electrodeposition step, the substrate was immersed into the permanganate solution for 35 min in order to allow solution penetration throughout the pores, achieving the gold surface. After electrodeposition, the polystyrene template was removed with tetrahydrofuran under stirring for 40 min. The obtained macroporous film was dried at vacuum and room temperature and characterized by FESEM and XANES.

Contact angle measurements

CA experiments were performed by slowly adding a 2 μL drop of $LiClO_4$ 0.5 mol L^{-1} aqueous solution over the film and measuring the angle formed between the air-solid and air-liquid lines. Each measurement was repeated three times.

Electrochemical characterization

CV measurements were performed between 0.0 V and 0.9 V (*vs.* Ag/AgCl, KCl_{sat}) in a $LiClO_4$ 0.5 mol L^{-1} aqueous solution as the electrolyte. As the counter-electrode, a 10 cm^2 platinum sheet was used.

Results and Discussion

Macroporous MnO_2 film characterization

According to the literature, MnO_2 films obtained by the electrochemical reduction of permanganate are

rather amorphous,[20] presenting good electrochemical performance,[21] and they are expected to be more stable when submitted to successive charge-discharge cycles due to easier structure accommodation. Besides, the development of MnO_2 by cathodic deposition allows the possibility of co-deposition and avoids the oxidation of the metallic substrate.[22]

Figure 1 shows Mn K-edge XANES experiments performed in order to elucidate the MnO_2 local structure compared with the spectra of standard MnO, Mn_2O_3, α-MnO_2 and δ-MnO_2. Manganese oxide exists in a wide range of structural forms and its electrochemical performance depends on its crystallographic form. δ-MnO_2 and α-MnO_2 are of particular interest due their opened structure.[15] Birnessite (δ-MnO_2) presents a 2D lamellar structure with large distance between the layers and Spinel (α-MnO_2) presents a 3D structure with interconnected tunnels allowing higher ionic diffusion of the electrolyte through the structure. For amorphous materials, in which the capacitance is mainly given by superficial processes, the surface area is the key factor in order to achieve a good performance.[23]

The sample presents, at the pre-edge region, two weak peaks at 6541 and 6543eV (inset at Figure 1a) corresponding to mixed Mn^{3+}/Mn^{4+} oxidation states. At the main-edge region, a sharp and intense peak at 6562 eV is present, corresponding to the dipole-allowed 1s→4p transition. This peak is related with a layered structure composed of MnO_6 octahedra edge-shared.[14,24] By comparing the sample spectra and the obtained from our standard materials and others shown in the literature,[25] it is possible to conclude that, although amorphous, the type and concentration of manganese sites is approximately the same in our sample and δ and γ-MnO_2.

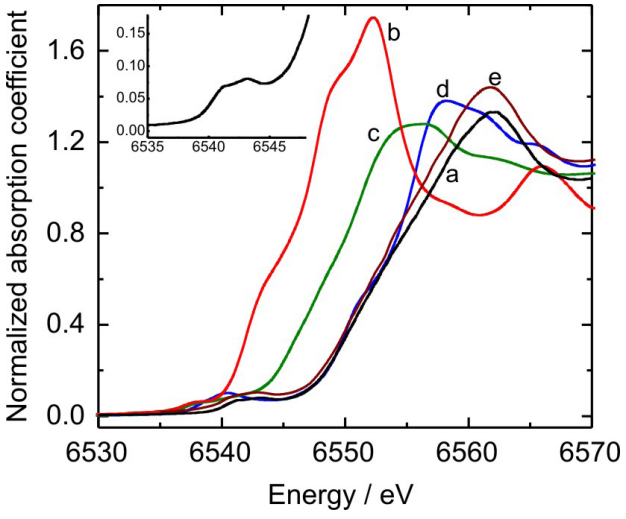

Figure 1. (color) Mn K-edge spectra of macroporous MnO_2 (black, a), MnO (red, b), Mn_2O_3 (green, c), α-MnO_2 (blue, d) and δ-MnO_2 (orange, e).

Figure 2 shows a FESEM image of a film obtained from template electrodeposition. It is possible to notice that highly porous and tridimensional films were formed with uniform covering of the substrate. The pores at the surface of the film present about the same diameter as the spheres used as a template (inset in Figure 2), which means that the film was grown at about the half of the spheres at the top of the film. From the images, it is also possible to observe the connections between the pores, seen as black holes at the bottom of the pores (also inset in Figure 2), which allow electrolyte penetration into the porous film.[26]

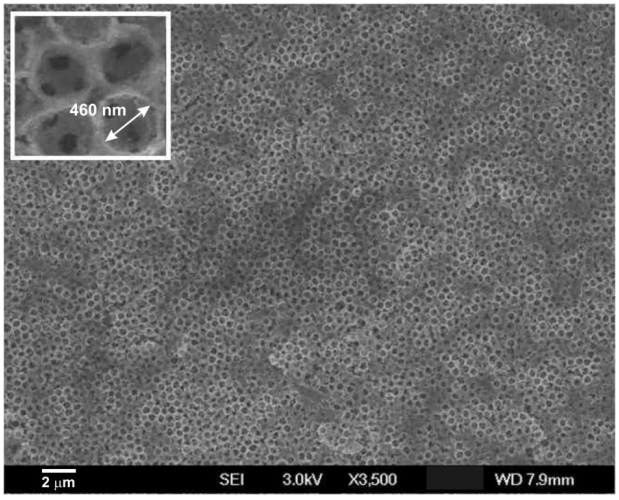

Figure 2. FESEM image obtained from MnO_2 films electrodeposited around 460 nm polystyrene spheres.

Wettability studies

When pores are used to increase the surface area for electrochemical applications, one must take into account wettability aspects because the electrolyte must penetrate into the pores in order to access all the electroactive material. To check this aspect, CA measurements were performed on both, a macroporous and a flat film obtained by electrodeposition at the same conditions, but without the spheres template. The values obtained were (88 ± 2)° and (36 ± 1)° for the macroporous and the flat film, respectively, which means that the liquid wets the flat surface better than the macroporous one.

The roughness of a surface affects its wettability[27-29] and depending on how this is affected, two different models can be applied. When a drop is placed onto a rough surface, it can fill the grooves (or pores) or stay on the surface, causing the formation of "air pockets". In the first case, the Wenzel's model is applied[30,31] and in the second one, the Cassie-Baxter's model is the most appropriated one.[32-34]

Both models can be used for the CA of rough surfaces, and the roughness geometry at the surface will define

which state is the most appropriate.[33] As the CA measured for macroporous surfaces are higher than for flat surfaces, the present system follows Cassie's regime. By analyzing this behavior from a different approach, the wettability is actually affected by the fraction of material in contact with the liquid.[35] When the liquid penetrates into the pores, at least at some level, the amount of material in contact with the liquid is higher than in the flat surface and the CA decreases, following Wenzel's model. When there is "air pocket" formation, the fraction of material in contact with the liquid decreases, increasing the CA, and Cassie's model can be applied.

Thermodynamically, the Wenzel model is expected for hydrophilic surfaces, like MnO_2, but experimentally it is possible to observe Cassie´s regime when there is air trapped inside the pores, which can be related to an energy barrier that avoids the transition from the Cassie situation to the Wenzel one. Abdelsalam *et al.*[36] suggested that this phenomena can be related to the small size (diameter < 1 μm) and geometry of the pores. However, Cassie's condition is metastable and can be changed into a Wenzel regime, which is the most stable one, through an external perturbation.[37]

Electrochemical characterization

Figure 3a shows the CV profile recorded at 0.09 V s^{-1} for the macroporous MnO_2 electrode in a $LiClO_4$ 0.5 mol L^{-1} aqueous electrolyte. It is possible to observe the typical supercapacitor rectangular shape, with no noticeable redox peaks. The same behavior has been observed at different scan rates (from 0.01 to 0.25V s^{-1}). In this case, fast, reversible and successive surface redox reactions occurs, making the shape of the voltammogram similar to that of double-layer type (i.e. carbon based supercapacitors).[38] The absence of peaks, corresponding to volumetric intercalation processes (when the redox reaction takes place in a deep portion of the film), is in agreement with a study performed by Ragupathy *et al.*[39] in which the surface redox reactions compensated by cation intercalation process (only in the outer portion of the film corresponding to a few hundred of Angstroms) is predominant in amorphous MnO_2 while the volumetric insertion/extraction process is predominant in crystalline MnO_2. So that, even that the voltammograms do not show current peaks, it does not mean that the material does not change its oxidation state.[40,41]

Specific capacitance (C) values have been calculated according to equation 1:

$$C = \frac{q}{v \times m} \quad (1)$$

Where *q* is the specific charge obtained by current *vs.* time curve integration, V is the voltage window and m is the mass of deposited material. At 0.04 V s^{-1}, the obtained C is 259 Fg^{-1}, which is a quite interesting value considering recent results reported for nanostructured MnO_2 films.[14,43,44] In an earlier contribution, Nakayama *et al.*[45] obtained macroporous MnO_2 films by template electrodeposition of approximately 740 nm pore diameter polystyrene nanospheres from a $MnSO_4$ aqueous solution, reporting on a KCl aqueous solution electrolyte with a C value of about half of that obtained in this work. These results show that, in order to obtain good electrochemical performance, several aspects must be taken into account, such as film preparation conditions and the electrolyte used.

For the flat electrode with approximately the same mass of deposited material, the obtained C is 100 Fg^{-1}, which is about 60% lower than that obtained with the macroporous film. This result shows that when the macroporous material is used, although the wettability is not as effective as it is for the flat electrode, the area in contact with the electrolyte is increased by introducing pores on the film at some level. Changes of wettabillity due to the electric field must ruled out in this case, because as the films are electroactive, the magnitude of the electric fields are very weak which is not the case when the films are insulating and lead to the phenomenon called "electro-wetting".[46] So that, another aspect that can contribute to higher capacitance of macroporous film is that, when the electrode is immersed into the electrolytic solution, the transition from Cassie's to the most thermodynamically stable Wenzel's state must occur, increasing the area in contact with the liquid.

When charge storage is governed by volumetric intercalation reactions, a strong dependence between capacity and scan rate is observed: with increasing scan rate, there is a capacity loss as a less deeper portion of bulk material will be involved in the process.[47] On the other hand, when the charge storage in mainly governed by a superficial mechanism, this dependence is not as pronounced, as only surface capacitive processes are involved. From Figure 3b, it can be observed that the C values slightly decrease by 20% when the scan rate is increased from 0.01 to 0.25 V s^{-1}. This result corroborates the predominant superficial mechanism contribution of macroporous MnO_2 film.

To investigate the MnO_2 macroporous film electrochemical stability, charge/discharge experiments have been performed by cyclic voltammetry at 0.04 V s^{-1}. Figure 4a shows the FESEM image of a film obtained from template electrodeposition in the same way as Figure 2, and it is possible to observe the same features. Figure 4b shows the capacity values obtained as a function of the cycle

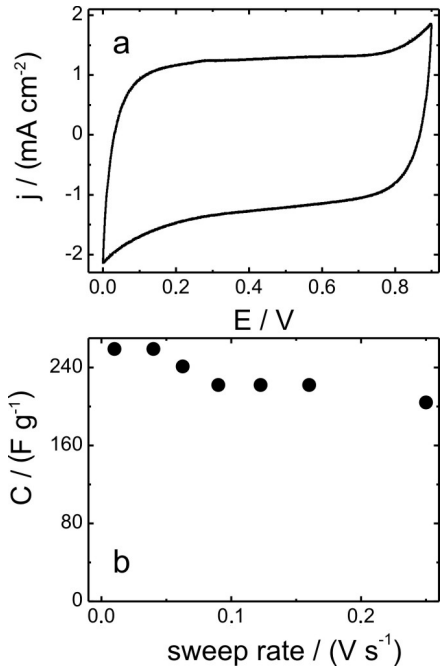

Figure 3. (a). j *vs.* E potentiodynamic profile at 90 mV s^{-1} and (b) Specific capacitance *vs.* v of MnO_2 macroporous films; electrolyte = 0.5 mol L^{-1} $LiClO_4$ aqueous solution; C.E. = Pt mesh; Ref. = Ag/AgCl 3 mol L^{-1} NaCl.

number. It is clear that the capacity values remain almost constant after 1000 cycles. Figure 4c shows that the pore structure at the surface of the film is maintained as well as the macroporous film morphology. This is a remarkable result considering that the electrode consists of only MnO_2 without any binder, such as PVDF, or electronic conductor, such as carbon black.

Conclusions

MnO_2 macroporous films were obtained by cathodic electrodeposition around polystyrene nanospheres. CA measurements have shown that the wettability of the macroporous film is lower than for the flat surface. However, the electrochemical response as a supercapacitor material presented an improvement of about 60% when compared with a flat MnO_2 electrode. This result demonstrates that, in spite of the wettability being lower, some penetration of the electrolyte into the pores must occur, increasing the electroactive area with respect to the flat electrode. Furthermore, the macroporous electrode showed excellent electrochemical stability, with neither a C decrease nor a loss of morphology, after 1000 cycles.

The introduction of pores into a film with the aim of increasing the surface area for electrochemical applications can be a good alternative. However, aspects concerning complete wetting of the film by the electrolyte are of great importance. Alternatives, like removal of air from the pores before the introduction of liquid or wetting by vapor condensation, can be applied in order to improve the electrode's wettability.

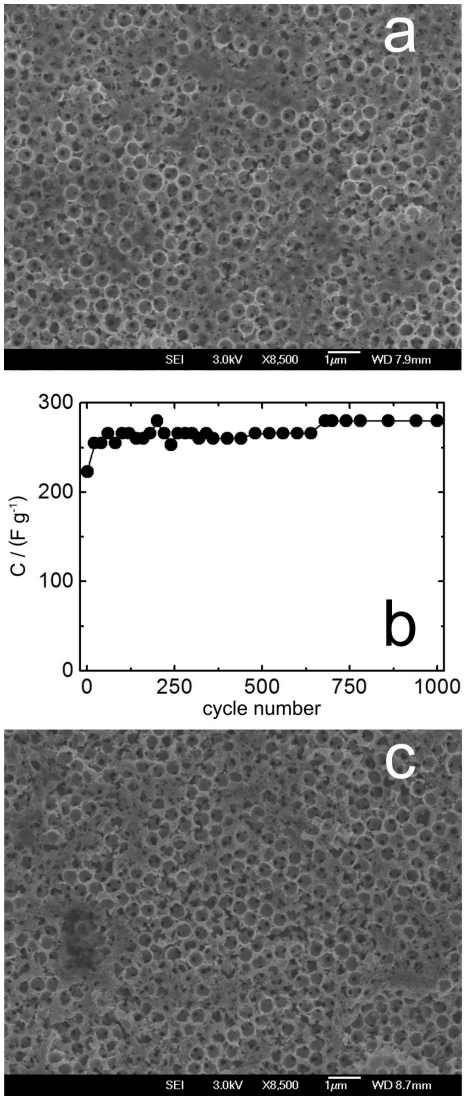

Figure 4. Specific capacitance as a function of cycle number (b), and FESEM images taken before (a) and after cycling (c). Electrolytic solution: $LiClO_4$ 0.5 mol L^{-1}, C.E. = Pt mesh; Ref. = Ag/ AgCl 3 mol L^{-1} NaCl.

Acknowledgment

The authors thank CNPq and CAPES for financial support. V. R. G. and T. M. B thank FAPESP for scholarships 05/59560-9 and 05/59135-6, respectively. LNLS (Campinas, Brazil) is gratefully acknowledged for absorption X-ray facilities.

References

1. Bazito, F. F. C.; Torresi, R. M.; *J. Braz. Chem. Soc.* **2006**, *17*, 627.

2. Aricò, A. S.; Bruce, P.; Scrosati, B.; Tarascon, J. M.; Van Schalkwijk, W.; *Nat. Mater.* **2005** , *4*, 366.
3. Simon, P.; Gogotsi, Y.; *Nat. Mater.* **2008**, *7*, 845.
4. Kötz, R.; Carlen, M.; *Electrochim. Acta* **2000**, *45*, 2483.
5. Soudan, P.; Gaudet, J.; Guay, D.; Bélanger, D.; Schulz, R.; *Chem. Mater.* **2002**, *14*, 1210.
6. Lee, H. Y.; Goodenough, J. B.; *J. Solid State Chem.***1999**, *144*, 220.
7. Benedetti, T. M.; Bazito, F. F. C.; Ponzio, E. A.; Torresi, R. M.; *Langmuir* **2008**, *24*, 3602.
8. Moser, F.; Athouël, L.; Crosnier, O.; Favier, F.; Bélanger, D.; Brousse, T.; *Electrochem. Commun.* **2009**, *11*, 1259.
9. Athoue, L.; Moser, F.; Dugas, R.; Crosnier, O.; Bélanger, D.; Brousse, T.; *J. Phys. Chem. B* **2008**, *112*, 7270.
10. Shinomiya, T.; Gupta,V.; Miura, N.; *Electrochim. Acta* **2006**, *51*, 4412.
11. Bordjiba, T.; Bélanger, D.; *J. Electrochem. Soc.* **2009**, *156*, A378.
12. Devaraj, S.; Munichandraiah, N.; *J. Phys. Chem. C* **2008**, *112*, 4406.
13. Machefaux, E.; Brousse, T.; Bélanger, D.; Guyomarda, D.; *J. Power Sources* **2007**, *165*, 651.
14. Ragupathy, P.; Park, D. H.; Campet, G.; Vasan, H. N.; Hwang, S. J.; Choy, J. H.; Munichandraiah, N.; *J. Phys. Chem. C* **2009**, *113*, 6303.
15. P. Simon, Y. Gogotsi, *Nat. Mater.*, **2008**, *7*, 845.
16. Gonçales, V. R.; Massafera, M. P.; Benedetti, T. M.; Moore, D. G.; Cordoba de Torresi, S. I.; Torresi, R. M.; *J. Braz .Chem. Soc.* **2009**, *20*, 663.
17. Bartlett, P. N.; Baumberg, J. J.; Coyle, S.; Abdelsalam, M. E.; *Faraday Discuss*. **2004**, *125*, 117.
18. Bartlett, P. N.; Baumberg, J. J.; Birkin, P. R.; Ghanem, M. A.; Netti, M. C.; *Chem. Mater.* **2002**, *14*, 2199.
19. Adamson, A. W. In *Physical Chemistry of Surfaces*; Adamson, A.; Gast, A. P. ed.; 5th ed., Wiley Interscience: New York, 1990, ch.10.
20. Wei, J.; Nagarajan, N.; Zhitomirsky, I.; *J. Mater. Process. Tech.* **2007**, *186*, 356.
21. Szamocki, R.; Velichko, A.; Mücklich, F.; Reculusa, S.; Ravaine, S.; Neugebauer, S.; Schuhmamm, W.; Hempelmann, R.; Kuhn, A.; *Electrochem. Commun.* **2007**, *9*, 2121.
22. Jacob, G. M.; Zhitomirsky, I.; *Appl. Surf. Sci.* **2008**, *254*, 6671.
23. Ghodbane, O.; Pascal, J. L.; Favier, F.; *Appl. Mater. Interfaces* **2009**, *1*, 1130.
24. Park, D. H.; Lee, S. H., Kim, T. W.; Lim, S. T.; Hwang, S. J.; Yoon, Y. S.; Lee, Y. H.; Choy, J. H.; *Adv. Funct. Mater.* **2007**, *17*, 2949.
25. Figueroa, S. J. A.; Requejo, F. G.; Lede, E. J.; Lamaita, L.; Peluso, M. A.; Sambeth, J. E.; *Catal. Today* **2005**, *107-108*, 849.
26. Hu, C. C.; Tsou, T. W.; *Electrochem. Commun.* **2002**, *4*, 105.
27. Patankar, N. A.; *Langmuir* **2003**, *19*, 1249.
28. Patankar, N. A.; *Langmuir* **2004**, *20*, 7097.
29. Quéré, D.; *Phys. A* **2002**, *313*, 32.
30. Wenzel, R. N.; *Ind. Eng. Chem. Res.* **1936**, *28*, 988.
31. Wolanski, G.; Marmur, A.; *Colloid Surf., A* **1999**, *156*, 381.
32. Cassie, A. B. D.; *Discuss. Faraday Soc.* **1948**, *3*, 11.
33. Cassie, A. B. D.; Baxter, S.; *Trans. Faraday Soc.* **1944**, *40*, 546.
34. Marmur, A.; Bittoun, E.; *Langmuir* **2009**, *25*, 1277.
35. Bico, J.; Marzolin, C.; Quéré, D.; *Europhys. Lett.* **1999**, *47*, 220.
36. Abdelsalam, M. E.; Bartlett, P. N.; Kelf, T.; Baumberg, J.; *Langmuir* **2005**, *21*, 1753.
37. Ishino, C.; Okumura, K.; Quéré, D.; *Europhys. Lett.* **2004**, *68*, 419.
38. Simon, P.; Gogotsi, Y.; *Nat. Mater.* **2008**, *7*, 845.
39. Ragupathy, P.; Vasan, H. N.; Munichandraiah, N.; *J. Electrochem. Soc.* **2008**, *155*, A34
40. Lee, H. Y.; Goodenough, J. B.; *J. Solid State Chem.* **1999**, *144*, 220.
41. Kuoa, S. L.; Wu, N. L., *J. Power Sources* **2006**, *162*, 1437
42. Sarangapani, S.; Tilak, B. V.; Chen, C. P.; *J. Electrochem. Soc.* **1996**, *143*, 3791.
43. Jiang, R.; Huang, T.; Liu, J.; Zhuang, J., Yu, A.; *Electrochim. Acta* **2009**, *54*, 3047.
44. Beaudrouet, E.; Le Gal La Salle, A.; Guyomard, D.; *Electrochim. Acta* **2009**, *54*, 1240.
45. Nakayama, M.; Kanaya, T.; Inoue, R.; *Electrochem. Commun.* **2007**, *9*, 1154.
46. Mugele, F.; Klingner, A.; Buehrle, J.; Steinhauser, D.; Herminghaus, S.; *J. Phys.: Condens. Matter* **2005**, *17*, S559.
47. Brousse, T.; Toupin, M.; Dugas, R.; Athouël, L.; Crosnier, O.; Bélanger, D.; *J. Electrochem. Soc.* **2006**, *153*, A2171.

Submitted: January 12, 2010
Published online: May 27, 2010

FAPESP has sponsored the publication of this article.